THERMAL DESIGN IMPROVEMENTS FOR 30kW$_e$ ARCJET ENGINES

88-073

W. D. Deininger,* A. Chopra,*
D. Q. King,# and T. J. Pivirotto*
Jet Propulsion Laboratory
California Institute of Technology
Pasadena, CA 91109

ABSTRACT

This paper describes two thermal design improvements for 30 kW$_e$ arcjet engines. A ZrB_2 high temperature coating was used to increase the surface emissivity of the nozzle radiating surface, enabling lower temperature operation, which should lead to longer nozzle life. The ZrB_2-coated engine operated about 120°C cooler than the uncoated baseline engine indicating a 30% increase in the surface emissivity. Additionally, a new engine design which has fewer active seals than previous designs and operates at lower overall component temperatures is described in detail. The nozzle on the new engine operated at a temperature of 1950°C at 30 kW$_e$ while the baseline engine nozzle reached 2000°C at 23 kW$_e$. In addition, the back of the new engine was more than a factor of two cooler when compared to the baseline engine.

NOMENCLATURE

NEP	Nuclear Electric Propulsion
SRPS	Space Reactor Power System
SP-100	100 kW$_e$ Space Reactor Power Source program
DACS	Data Acquisition and Control System
LVDT	Linear Voltage Displacement Transducer
V-I	Voltage-Current Characteristics
I_A	Arc Current
V_A	Arc Potential
$\dot{m}$	Propellant Mass Flow Rate
P_E	Engine Input Power
P_S	Specific Power, $P_E/\dot{m}$
T_B	Brightness Temperature

INTRODUCTION

Active research on thermal arcjet thrusters, begun during the late 1950s and pursued vigorously until the mid-1960s, is reviewed in References 1 and 2. During that period, arcjet engines were being developed for primary propulsion applications powered by Space Reactor Power Systems (SRPS). Engines requiring from one kilowatt to more than 200 kW$_e$ of input power were examined. Engine operation on a variety of propellant gases was investigated, including H_2, He, Li, N_2, NH_3, N_2H_4, Ne and Ar. Development of both high-power solar and nuclear space power systems (particularly the SP-100 SRPS program) has renewed interest in using electric propulsion for primary propulsion functions and has led to renewed development of arcjet engines.

An ammonia arcjet engine was operated for 573 hours during a recent long-duration test.[3-5] This arcjet will be referred to as the "baseline engine" for the purposes of this paper. The engine was based on a design originally tested for 50 hours in 1964, the previous endurance record for ammonia arcjet operation.[6] Tungsten whisker growth on the cathode tip caused a low voltage condition in the engine, terminating the long-duration test.[4,5,7] The 573-hour endurance test served as a means of re-establishing arcjet engine technology, which had received little attention since the middle 1960s due to a lack of adequate space-based power.

A schematic of a typical arcjet engine configuration is shown in Fig. 1. It consists of a one piece plenum chamber-constrictor-expansion nozzle which also forms the discharge anode. The cathode is a conically-tipped rod centrally located in the plenum chamber near the constrictor entrance. An insulator holds the cathode in place and isolates the two electrodes. The propellant gas is fed into the plenum chamber tangentially, is heated by passing through and around an arc discharge and is then expanded in a supersonic nozzle to produce thrust. After the engine is started, a constricted arc extends from the conical tip of the cathode through the constrictor and attaches to the small end of the nozzle as shown in Fig. 1. The conical tip of the cathode provides a high temperature region for thermionic emission of electrons. The arc is blown downstream through the constrictor channel by the propellant gas pressure in the plenum chamber. The attachment point in the nozzle must be either diffuse or, if concentrated, must move very rapidly within the nozzle to prevent anode surface melting. The propellant receives the bulk of the thermal energy in a thin cylinder along the center line of the constrictor.

One of the major operational problems of radiation-cooled thermal arcjet engines stems from the high temperatures at which the thruster components must operate. Thermal analysis done by Avco Corporation affords insight into the limiting temperatures, temperature gradients and heat flow paths that the arcjet nozzle block must be capable of withstanding for long periods.[8] The results of these calculations are shown in Fig. 2. Note that there is some natural regenerative cooling since about 10% of the total engine power is conducted from the hot expansion nozzle back to the cooler propellant plenum chamber heating the incoming propellant. The maximum nozzle surface temperature appears to occur at the arc attachment area and can be as high as 2500 K for an engine input power of 30 kW$_e$.[8]

These high engine temperatures have led to operational problems during engine testing. Historically, the first major problem encountered was electrode and seal failure from overheating.

---

* Member Technical Staff, Electric Propulsion and Plasma Technology Group, Propulsion Systems Section. Member AIAA.

\# Supervisor, Electric Propulsion and Plasma Technology Group, Propulsion Systems Section. Member AIAA.

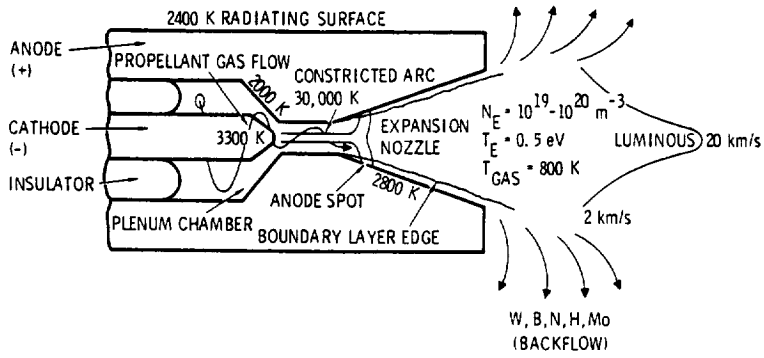

Figure 1. General Schematic of Arcjet Engine Operation.

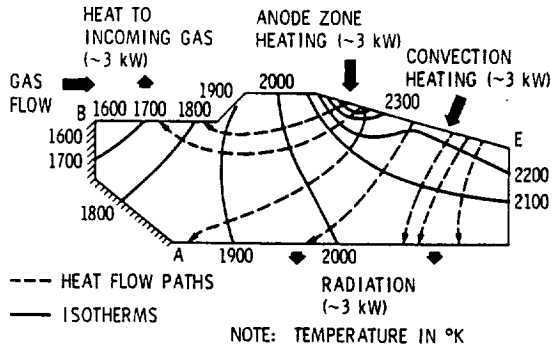

Figure 2. Results of Heat Transfer Calculations in the Nozzle Block of a 30 kW_e engine (Ref. 8).

Overheating can also induce evaporation of electrode material and result in a shorter electrode life. Overheating of other engine parts such as joints, seals and insulators can cause propellant leaks and could lead to engine failure.

This paper discusses experimental results which indicate thermal design improvements for 30 kW_e arcjet engines and compares these results to the thermal characteristics of the baseline engine. A technique to increase the emissivity of the nozzle radiating surface is described first. This involves coating the outer surface of the nozzle with a high temperature, high emissivity material to enhance radiative cooling. In addition, a new engine design is described in detail; this design incorporates improved regenerative cooling and has fewer high temperature seals than the baseline engine.

FACILITIES AND INSTRUMENTATION

The tests described in this paper were conducted in a water-cooled, cylindrical, stainless steel vacuum tank 1.2 m in diameter and 2.1 m long. The exhaust plume of the arcjet was collected by a water-cooled diffuser, 0.16 m in diameter, and pumped by a vacuum pumping plant based on a 6.3 m^3/s roots blower. Tank pressures were maintained between 0.04 and 0.07 torr (5.3 to 9.3 Pa) during engine operation.

Engine operation and the facility were monitored by a computer-based, Data-Acquisition and Control System (DACS).[12,13] Measurements of the arc current, arc voltage, propellant flow rate, tank pressure, and various engine and facility temperatures were taken at each propellant flow rate and power setting. These parameters were recorded every 20 s by the computer-based DACS. This system also computed the input power in real time. Once the engine reached steady-state operating conditions, typically 10 to 15 minutes, several sets of operational data were recorded and then operating conditions were changed to prepare for the next set of data. Detailed descriptions of the test facility and instrumentation can be found in References 4 and 5.

The infrared optical pyrometer which monitored the nozzle temperature used a room temperature silicon detector element, had a spot size of 0.64 cm and operated in the wavelength range of 0.6 to 1.0 micrometers. The emissivity of tungsten, see Fig. 3, is relatively insensitive to temperature in this wavelength range.[9] The pyrometer was located outside of the vacuum tank and viewed the engine through a 1.9 cm thick glass window. A National Bureau of Standards tungsten ribbon filament lamp was used to calibrate this system. The lamp was located inside the vacuum tank at the position occupied by the engine. The known lamp brightness temperature was then used to correct the pyrometer data with a systematic uncertainty of $\pm 6^0$C. Type K thermocouples were used to monitor the temperatures at the rear of the engine.

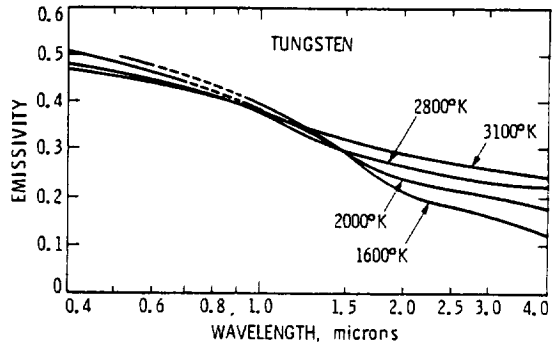

Figure 3. Normal Emissivity of Tungsten (Ref. 9).

ARCJET ENGINE DESIGNS

Several arcjet engine designs were evaluated during the course of these tests. The essential dimensions

and critical parameters of these engines are summarized in Table 1. The baseline engine was identical to the engine used in the 573-hour duration test program. The "baseline MOD-III" engine incorporated a high emissivity coating on the nozzle radiating surface of the baseline engine. The "D-1E" engine is a new design with fewer seals and improved regenerative cooling and is described in detail and compared to the baseline engine.

TABLE 1. Design Parameters and Essential Dimensions of the Engines Used in These Experiments.

PARAMETER	BASELINE ENGINE	MOD-III ENGINE	D-1E ENGINE
Constrictor Length, cm	1.07	1.07	1.08
Constrictor Diameter, cm	0.51	0.51	0.50
Nozzle Exit Diameter, cm	2.41	2.41	2.93
Exit Area Ratio+	23	23	33
Nozzle Type	38° cone	38° cone	bell
Outer Nozzle Surface Material	W	ZrB_2	W
Plenum Chamber Diameter, cm	2.03	2.03	2.03
Plenum Half Angle Taper at Constrictor End	50°	50°	49.5°
Cathode Diameter, cm	0.95	0.95	0.95
Cathode Tip Included Angle	60°	60°	60°
Cathode Tip Radius, cm	0.15	0.15	0.15
Electrode Gap*, cm	0.21	0.21	0.21
Propellant Injection Angle	30°	30°	30°
Nominal Engine Diameter, cm	5.08	5.08	5.08
Nominal Engine Length, cm	14.7	14.7	15.0

+ Ratio of constrictor area to nozzle exit area.
* Axial gap between the cathode cone and corner of the constrictor entrance.

Baseline Engine

A schematic drawing of the baseline arcjet engine used for these experiments is shown in Fig. 4. The engine design is summarized here in terms of the features important to its thermal behavior. Additional details can be found in References 3 through 5. The plenum chamber-constrictor-supersonic nozzle was turned from a single piece of 2% thoriated tungsten. The plenum chamber has a diameter of 2.03 cm and has a 50° half-angle taper to the constrictor which has a diameter of 0.51 cm and a length of 1.07 cm. The nozzle has an area ratio of 22 and takes the form of a 19° half-angle cone. The nozzle block has a 7° taper along its back edge and is fitted into a cylindrical molybdenum body, as shown in Fig. 4. Lapping these parts together at the 7° taper effects a gas-tight seal between the engine body and nozzle block.

The ammonia propellant is fed into the engine through a stainless steel tube welded into a flange made of Inconel 600 on the side of the engine body, as shown in Fig. 4. A cylinder of boron nitride with a square, helical groove machined in its outer surface forces the incoming propellant to flow along the hot inner surface of the molybdenum body to reduce the heat flow to the seals at the rear of the engine. A small amount of propellant also flows between the boron nitride cylinder and the cathode.

The back end of the engine is closed with a 1.91 cm thick disk of boron nitride. A standard swaglock bulkhead fitting/feedthrough seals the cathode at the boron nitride disk. A 2.54 cm diameter by 0.25 cm thick stainless steel washer is welded to the fitting, as shown in Fig. 4, to increase the bearing surface on the boron nitride.

A split ring of titanium engages the molybdenum body through a matching groove machined into the molybdenum as is shown in Fig. 4. Eight 0.64 cm diameter threaded molybdenum rods running through the boron nitride disk, Inconel flange and titanium retaining ring hold the engine together. Gaskets of 0.08 cm thick pure graphite are used as seals in four places as shown. This material is capable of sealing up to a temperature of 3316°C in an inert atmosphere.[10] The steel nuts on the eight rods required tightening after each run since the boron nitride, Inconel, and titanium expanded more than the molybdenum rods/steel nuts causing the nuts to creep and the joints to become loose after engine cool down.

Baseline MOD-III Engine

The baseline MOD III engine is identical to the Baseline engine (Fig. 4) except that it was plasma spray coated, with 325 mesh size ZrB_2, on the outer nozzle and body surfaces as shown in Fig. 5. The coating had a thickness of 0.025 cm and had a mat grey appearance at room temperature. Emissivities ranging from 0.50 to 0.95 are reported in the literature for ZrB_2.[11]

D-1E Engine

A schematic drawing of the D-1E engine used for these experiments is shown in Fig. 6. The plenum chamber-constrictor- supersonic nozzle was again turned from a single piece of 2% thoriated tungsten. The constrictor has a diameter of 0.50 cm and a length of 1.08 cm and the plenum chamber has a diameter of 2.03 cm and a 49.5° half-angle taper at the constrictor end. This engine has a contoured nozzle which was defined by Brophy, et. al.[12] to improve the arcjet nozzle efficiency.[13,14] This nozzle has an exit diameter of 2.93 cm and an area ratio of 33. This nozzle block is also fitted into a cylindrical molybdenum body. However, the 7° taper on the D-1E engine nozzle block is placed 2.82 cm in front of the rear edge, as shown in Fig. 6. Again, a gas-tight seal was effected between the tungsten and molybdenum by lapping the parts together at the 7° taper.

The engine is held together by threading the 6.35 cm diameter molybdenum assembly nut onto the threaded end of the molybdenum body. This nut holds the boron nitride insulator in place which closes the back of the engine. A lip on the back of the assembly nut presses a stainless steel spacer against the boron nitride insulator which, in turn, compresses the 0.15-cm thick pure graphite gasket material against the back of the molybdenum body to provide a gas-tight seal, see Fig. 6. The stainless steel spacer is required because the molybdenum expands more than the boron nitride at high temperatures which would reduce pressure on the graphite gaskets. The stainless steel spacer provides adequate expansion to maintain the gasket pressure.

The ammonia propellant is fed into the engine through a stainless steel tube welded into the side of an Inconel 600 feedthrough at the back of the engine as shown in Fig. 6 instead of on the side of the engine as in the baseline design. A swaglock bulkhead fitting is welded to the Inconel 600 feedthrough for a seal on the cathode. The Inconel 600 feedthrough is sealed against the boron nitride insulator with pure graphite gasket material, 0.15-cm thick, by tightening an Inconel 600 nut and thick washer against the inner surface of the boron nitride. The propellant flows through an annulus 0.12 cm wide between the cathode surface and the inside diameter of the Inconel 600 feedthrough into a small plenum cavity. Then, as with the baseline engine, the propellant flows along the hot inner surface of the molybdenum body through a square spiral propellant groove machined into the outer surface of a cylinder of boron nitride. A small amount of propellant also flows between the boron nitride cylinder and the cathode. The boron nitride pieces are stepped in

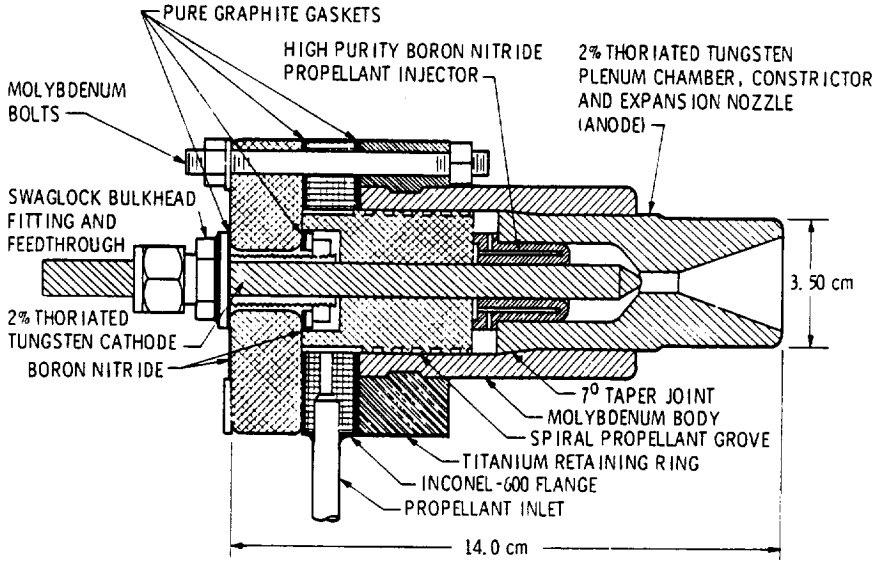

Figure 4. Schematic of Baseline Arcjet Engine.

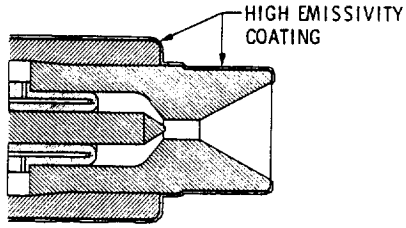

Figure 5. Baseline MOD-III Engine.

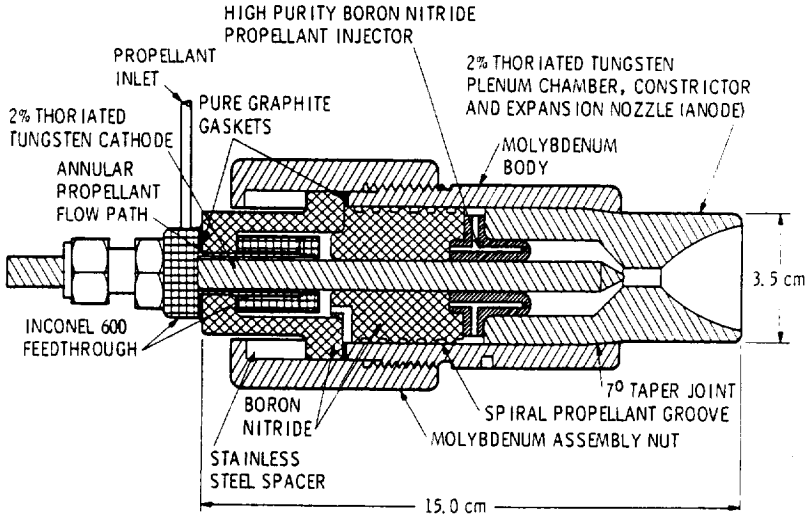

Figure 6. Schematic of D-1E Arcjet Engine.

the D-1E engine to prevent a line-of-site discharge path between the insulator pieces for arcs between the electrodes.

A cylindrical insulator made of high purity (high temperature) boron nitride serves as the propellant injector and holds the cathode concentric to the constrictor and plenum chamber as in the baseline design. Propellant is injected into the plenum chamber through four 0.15 cm diameter holes drilled through the high purity boron nitride. The downstream ends of these four holes are at an angle of 60° to the plane of Fig. 6. In this way the propellant in both engine designs is injected tangentially into the plenum chamber at a radius of 0.75 cm and with a downstream inclination of 30°. However, the injector block in the D-1E engine extends 1.2 cm along the inside of the engine body compared to 1.9 cm for the baseline engine. This moves the insulator face further away from the discharge to reduce its thermal load. Again, the upstream end of the injector is stepped to prevent a line-of-site discharge path between the insulator pieces.

The cathode, identical to that used in the baseline engine, is made of 2% thoriated tungsten, is 0.95 cm in diameter and is 18 cm long. It has a 60° included angle tip with a 0.15 cm radius point. The minimum gap between the cathode cone and the constrictor entrance is 0.21 cm.

EXPERIMENTAL RESULTS AND DISCUSSION

Results of experiments describing arcjet engine operation with a high emissivity nozzle coating and operation of the new engine design are described below.

HIGH EMISSIVITY COATING EXPERIMENTS

ENGINE OPERATING CHARACTERISTICS The V-I characteristics are the same for both the baseline and baseline MOD III engines and are shown in Fig. 7. Knowledge of the engine V-I characteristics is important when discussing engine thermal behavior since anode heating is driven in part by current collection through the anode sheath. The solid lines represent constant mass flow, while the dashed lines are for constant power.

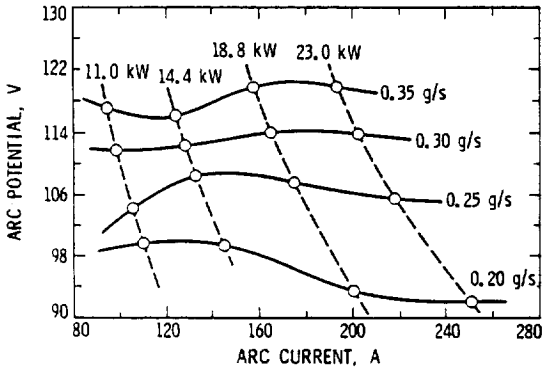

Figure 7. Baseline Engine Voltage-Current (V-I) Characteristics.

NOZZLE TEMPERATURE REDUCTION TESTS Comparisons of the indicated nozzle surface brightness temperature, at a point 1 cm upstream of the nozzle exit plane of the baseline engine, before and after coating with ZrB_2, are shown in Figs. 8a and b. At mass flow rates of 0.25 g/s and 0.30 g/s, the ZrB_2-coated engine (baseline MOD III) operated about 120°C cooler over the power range considered. This result indicates a 35% increase in surface emissivity at 1800°C as obtained from the Stefan-Boltzmann law by assuming a constant radiated power for both engines. A constant radiated power is assumed since the engine is run at the same mass flow rate and power (same voltage-current characteristic) both before and after coating with ZrB_2; the only modification made to the engine is the increase in the radiating surface emissivity. As mentioned earlier, the reported emissivity of tungsten is about 0.4 (see Fig. 3) and that of ZrB_2 ranges from 0.5 to 0.95. The results presented in this paper suggest that the emissivity of ZrB_2 is about 0.55.

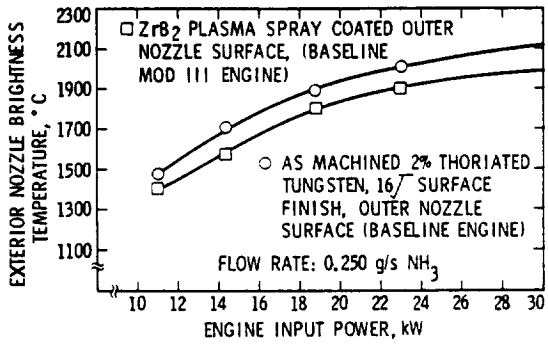

Figure 8a. Nozzle Brightness Temperature as a Function of Power for a Mass Flow Rate of 0.25 g/s With and Without the ZrB_2 Coating.

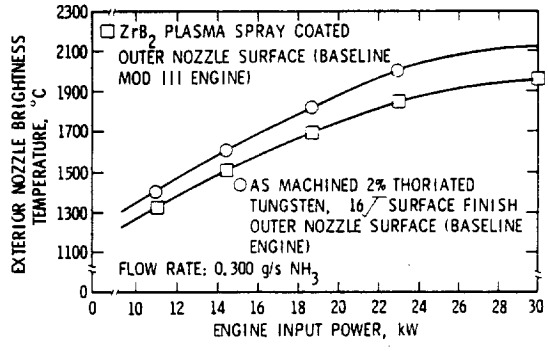

Figure 8b. Nozzle Brightness Temperature as a Function of Power for a Mass Flow Rate of 0.30 g/s With and Without the ZrB_2 Coating.

The engine was run at powers ranging from 10.0 kW to 37.0 kW and mass flow rates of 0.20 g/s to 0.35 g/s to characterize the performance of the coating. Further details on the operating characteristics and performance of the baseline engine design can be found in the references.[3-5] The coated baseline engine was run for more than 30 hours at different powers and flow rates and subjected to numerous start sequences with no apparent change in the ZrB_2 coatings mechanical properties or high temperature optical properties.

The mat grey room temperature appearance of the ZrB_2 coating took on a yellowish tint following engine operation on both the tungsten nozzle and molybdenum body substrates. It should be noted that this coating has also been applied to the molybdenum anode block of an MPD thruster being run on argon propellant. The molybdenum MPD anode operates in the same temperature regime as the

molybdenum arcjet body. However, in the case of the MPD thruster, no coating color change was evident. Therefore, it is believed that the ZrB_2 coating is undergoing a mild chemical reaction with the ammonia propellant when it is cold flowed prior to a test and/or with the dissociated ammonia products created by arcjet operation. The long term effects of this process still need to be determined.

VERIFICATION OF D-1E ENGINE THERMAL DESIGN

Tests were conducted to examine the temperatures of the D-1E engine at various locations. As above, the bare tungsten nozzle surface temperature, at a point 1 cm upstream of the nozzle exit plane, was continuously measured with an infrared optical pyrometer. Two type K thermocouples were attached to the engine to monitor engine component temperatures which could not be measured with the optical pyrometer since they were below its lower sensitivity limit of 1200°C. Referring to Fig. 6; one of these thermocouples was spot-welded to the side of the Inconel 600 feedthrough 90° from the propellant inlet tube; the other was clamped onto the side of the molybdenum assembly nut about 1 cm from the back of the engine.

ENGINE OPERATING CHARACTERISTICS The D-1E engine voltage-current (V-I) characteristics are shown in Fig. 9. Again, the solid lines represent constant mass flow, while the dashed lines represent constant power. This characteristic is similar to that of the baseline engine.

The V-I characteristic shown in Fig. 9 should be compared to that shown in Fig. 10 for the baseline MOD-I engine, taken from Reference 14. The same constant power and constant mass flow rate characteristics are exhibited for both engine designs; however, for constant power and flow rate, the D-1E engine operates at a voltage 10% lower than the baseline MOD-I engine. This difference is believed to occur since the D-1E engine expands less than the baseline MOD I engine resulting in a smaller minimum gap between the cathode cone and constrictor inlet making the arc shorter and reducing the operating voltage. Reference 14 describes baseline MOD-I engine operation in detail. The baseline MOD-I engine incorporates a bell-shaped nozzle on the baseline engine which is identical to the bell-shaped nozzle on the D-1E engine.

THERMAL DESIGN RESULTS The D-1E engine was operated over a power range of 13.2 to 30.4 kW_e and mass flow rates of 0.20, 0.25 and 0.30 g/s to characterize its thermal design. The exterior engine temperature at the three locations discussed above is shown in Fig. 11 as a function of electrical input power for constant mass flow rate.

As can be seen in Fig. 11, the nozzle brightness temperature increases with increasing input power and is in general substantially lower for the D-1E engine as compared to the baseline engine. For example, at a mass flow rate of 0.3 g/s and a power of 23 kW_e, the D-1E engine had a nozzle temperature of about 1750°C while the baseline engine operated with a nozzle temperature of 1970°C. This results primarily from the location of the 7° taper joint where the nozzle block and engine body are in intimate contact. This joint is at the front edge of the engine body on the D-1E engine as opposed to being several centimeters back from the front edge as on the baseline engine. As a result, the taper is closer to the nozzle heat source in the D-1E engine and conducts more heat into the engine body effecting a larger nozzle radiating surface.

In addition, in the baseline engine the nozzle was forced to radiate energy directly to the engine body inner surface for about half its length before

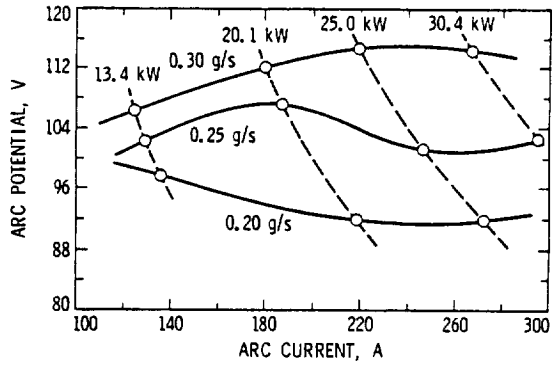

Figure 9. D-1E Engine Voltage-Current (V-I) Characteristics.

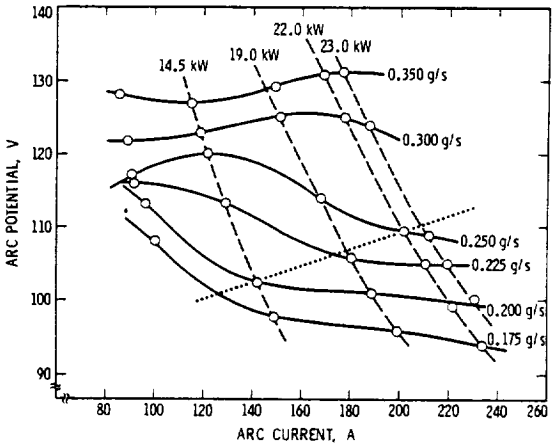

Figure 10. Baseline MOD I Engine Voltage-Current (V-I) Characteristics (Ref. 14).

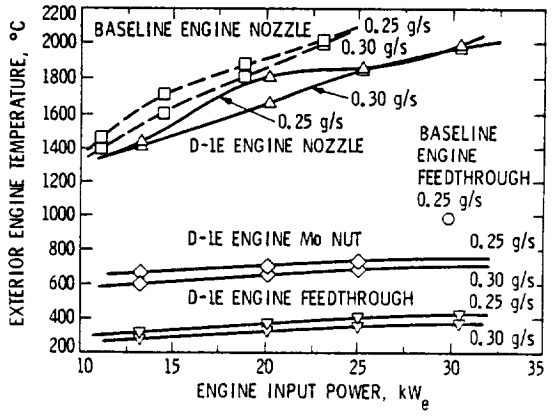

Figure 11. Exterior Engine Temperature as a Function of Input Power for Constant Mass Flow Rate.

reaching the direct conduction path at the 7° taper joint. In the D-1E engine the 7° taper joint is encountered first, producing a more effective radiative design. It should also be noted that the D-1E engine runs with a cooler nozzle block then the baseline MOD-I engine described in Ref. 14, even though the D-1E engine requires more current

to run at the same power. Assuming that the anode fall is constant with respect to current means that the D-1E engine incurs a higher anode heat load then the baseline MOD I engine. Even so, the nozzle temperature is lower. Therefore, two features, an improved thermal conduction path and more effective radiative design, provide a reduced nozzle temperature in the D-1E engine.

At an ammonia mass flow rate of 0.25 g/s and a power of 30 kW_e the baseline engine cathode feedthrough reached a temperature of about 1000°C while the D-1E engine feedthrough temperature measured only 425°C (see Fig. 11). This results from the fact that the cathode is cooled directly by the cold incoming propellant gas in the D-1E engine (see Fig. 6). There is no active cathode cooling at the back of the baseline engine (see Fig. 4). This regenerative cathode cooling maintains the feedthrough at a temperature far below the material thermal yield point.

Also shown in Fig. 11 are the temperature characteristics for the molybdenum assembly nut and Inconel feedthrough at the back of the engine. These quantities are important since heat at the back of the engine could be conducted into the host spacecraft in a flight system. Both of these parts exhibited relatively small temperature increases with increasing input power and decreasing mass flow rate. For example, the temperature of the assembly nut increased 2.8% for a corresponding power increase of 20%, or a 20°C increase in temperature for a 4.9 kW_e power increase. The Inconel feedthrough temperature increased from 348°C to 396°C when the mass flow was decreased from 0.30 g/s to 0.25 g/s at an engine power of 25.0 kW_e.

The exterior nozzle temperature is plotted as a function of specific power in Fig. 12. The specific power, P_S, is defined as the engine input power, P_E, divided by the mass flow rate, $\dot{m}$. As can be seen, each pair of curves in Fig. 11 are reduced to a single curve. Engine temperature rises as specific power increases. The temperature rise is linear for the components at the back of the engine and is non-linear for the nozzle temperature increase. The D-1E engine nozzle operates at a lower temperature for a given specific power than the baseline engine.

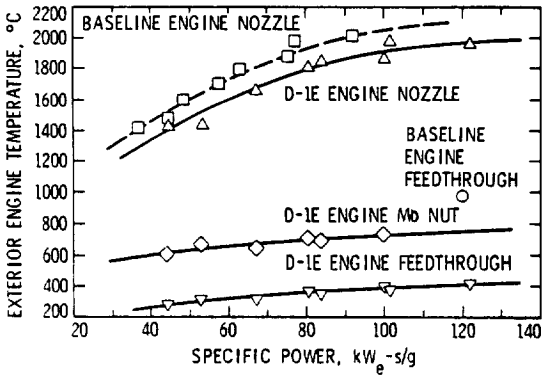

Figure 12. Exterior Engine Temperature as a Function of Specific Power (kW_e·s/g).

CONCLUSIONS

This paper described thermal design improvements for 30 kW_e arcjet engines. A ZrB_2 high temperature coating was used to increase the surface emissivity of the nozzle and body radiating surfaces enabling lower temperature operation which should lead to longer nozzle life. The ZrB_2-coated engine operated about 120°C cooler than the uncoated baseline engine over the power range considered indicating a 30% increase in the surface emissivity. This coating material maintained its high temperature optical properties over more than 30 hours of engine operation at different power levels and flow rates, including numerous start sequences.

A new engine design has been described in detail which has fewer active seals and parts than previous designs. The new engine assembly procedure is simpler and allows easier alignment than that of the baseline engine since there are no bolts. In addition, the seals at the back of the engine do not loosen up after engine cool down as was the case with the baseline engine. The new engine design will make future parametric testing simpler since the complexity of parts changeout is reduced.

The new engine design operates at lower overall component temperatures than previous designs. The nozzle operated at a temperature of 1950°C at 30 kW_e on the new engine while reaching 2000°C at 23 kW_e using the baseline design. This resulted from an improved conduction path leading to a larger effective radiator surface and a more efficient radiator surface design. In addition, the back of the new engine was more than a factor of two cooler when compared to the baseline engine due to improved regenerative cathode cooling.

ACKNOWLEDGEMENTS

The research described in this paper was carried out by the Jet Propulsion Laboratory (JPL), California Institute of Technology, and was sponsored by the Strategic Defense Initiative Organization, Innovative Science and Technology Office, and the National Aeronautics and Space Administration. The work was performed as part of JPL's Center for Space Microelectronics Technology.

The authors would like to thank W. R. Thogmartin, R. L. Toomath, and A. G. Owens for facilities and electronics support.

REFERENCES

1. L.E. Wallner and J. Czika, Jr., Arcjet Thruster for Space Propulsion, NASA TN D-2868 (June 1965).

2. T.J. Pivirotto and D.Q. King, "Thermal Arcjet Technology for Space Propulsion," JANNAF Propulsion Meeting, San Diego, California (Spring 1985).

3. T.J. Pivirotto, D.Q. King, W.D. Deininger, and J.R. Brophy, "The Design and Operating Characteristics of a 30 kW Thermal Arcjet Engine for Space Propulsion," 22nd JPC, AIAA Paper 86-1508 (June 1986).

4. T.J. Pivirotto, D.Q. King and W.D. Deininger, "Long Duration Test of a 30-kW Class Thermal Arcjet Engine," 23rd JPC, AIAA Paper 87-1947 (June 1987).

5. T.J. Pivirotto, D.Q. King, J.R. Brophy, and W.D. Deininger, Performance and Long Duration Test of a 30-kW Class Thermal Arcjet Engine, Final Report, AFAL-TR-87-010, JPL D-4643, (For the Air Force Astronautics Laboratory, Edwards AFB) (July, 1987).

6. R.R. John, Thirty-Kilowatt Plasmajet Rocket Engine Development, Summary Report, AVCO Corporation, RAD TR-64-6, NASA CR-54044 (July 1964).

7. T.J. Pivirotto and W.D. Deininger, "Analysis of a used pair of arcjet engine electrodes," SPIE Paper 872-11, SPIE Proceedings Volume 872, (January 1988), pp. 119-126.

8. R.R. John, S. Bennett, M. Chen, and J.F. Connors, "Arcjet Engine Performance: Experiment and Theory," ARS, Paper No. 2667-62 (1962).

9. T. Riethof, B. D. Acchione and E. R. Branyan, "High-Temperature Spectral Emissivity Studies on Some Refractory Metals and Carbides," Art. 49, Temperature, Vol. 3, A. I. Dahl, edt., Reinhold Publishing, New York, 1962. pp. 515-522.

10. Union Carbide Corporation, Carbon products Division, Chicago, Illinois, GRAFOIL® Catalog G-8816.

11. Handbook of Thermophysical Properties of Solid Materials, (MacMillan Company, New York) 1961.

12. J.R. Brophy, T.J. Pivirotto, and D.Q. King, "Investigation of arcjet nozzle performance," 18th IEPC, AIAA Paper 85-2016 (October 1985).

13. W.D. Deininger, T.J. Pivirotto, and J.R. Brophy, "The design and Operating Characteristics of an advanced 30-kW Ammonia Arcjet Engine," 19th IEPC, AIAA Paper 87-1082 (May 1987).

14. W.D. Deininger and T.J. Pivirotto, "Detailed operating characteristics of a 30 kW ammonia arcjet engine with a bell shaped nozzle," SPIE Paper 872-10, SPIE Proceedings Volume 872, (January 1988), pp. 108-118.